LM-02K092
September 19, 2002

Lattice-Matched GaInAsSb/A1GaAsSb/GaSb Materials for Thermophotovoltaic Devices

C.A. Wang, C.J. Vineis, H.K. Choi, M.K. Connors, R.H. Huang, L.R. Danielson,
G. Nichols, G.W. Charache, D. Donetsky, S. Anikeev, G. Belenky

NOTICE

This report was prepared as an account of work sponsored by the United States Government. Neither the United States, nor the United States Department of Energy, nor any of their employees, nor any of their contractors, subcontractors, or their employees, makes any warranty, express or implied, or assumes any legal liability or responsibility for the accuracy, completeness or usefulness of any information, apparatus, product or process disclosed, or represents that its use would not infringe privately owned rights.

1- 02K092
MS-1575

Lattice-Matched GaInAsSb/AlGaAsSb/GaSb Materials for Thermophotovoltaic Devices

C.A. Wang, C.J. Vineis*, H.K. Choi#, M.K. Connors, R.H. Huang
Lincoln Laboratory, Massachusetts Institute of Technology, Lexington, MA 02420-9108
**now at AmberWave Systems Corporation, Salem, NH 03079*
#now at Kopin Corporation, Taunton, MA 02780

L.R. Danielson, G. Nichols, G. W. Charache+
Lockheed Martin, Inc., Schenectady, NY 1230
+now at Princeton Lightwave, Cranberry, NJ 08512

D. Donetsky, S. Anikeev, G. Belenky
State University of New York, Stony Brook, NY 11794-2350

ABSTRACT

High-performance GaInAsSb/AlGaAsSb/GaSb thermophotovoltaic (TPV) devices with quantum efficiency and fill factor near theoretical limits and open-circuit voltage within about 15% of the limit can be routinely fabricated. To achieve further improvements in TPV device performance, detailed materials studies of GaInAsSb epitaxial growth, the microstructure, and minority carrier lifetime, along with device structure considerations are reported. This paper discusses the materials and device issues, and their implications on TPV device performance. In addition, improvements in TPV performance with integrated distributed Bragg reflectors and back-surface reflectors are discussed.

INTRODUCTION

Recently, a thermodynamic analysis of TPV system performance reported the importance of below-bandgap photon recuperation in determining tradeoffs between thermophotovoltaic (TPV) system efficiency and power density[1]. The maximum efficiency depends on both the bandgap of TPV cells and the reflectivity of the below-bandgap filter. It was shown that the bandgap where the efficiency is a maximum decreases as the reflectivity of the filter decreases. For TPV systems with hot-side operating temperatures of approximately 1000 °C and a 95% reflective filter, a maximum efficiency is predicted for TPV devices with a bandgap of 0.5-eV. GaInAsSb quaternary alloys lattice matched to GaSb have bandgaps that can be tailored from about 0.3 to 0.7 eV, and therefore are attractive alloys for these TPV systems[2].

Consequently, the development of GaInAsSb TPV devices has been ongoing for several years, and devices have been demonstrated using structures prepared by all the major epitaxial technologies, including liquid phase epitaxy[3-4], molecular beam epitaxy[5-6], and organometallic vapor phase epitaxy (OMVPE)[6-9]. A performance factor used for

*This work was sponsored by the Department of Energy under Air Force Contract No. F19628-00-C-0002. The opinions, interpretations, conclusions and recommendations are those of the author and are not necessarily endorsed by the United States Government.

overall TPV device evaluation is the diode efficiency[1] η_{diode}, which is given by $\eta_{diode} = QE*F_0*(qV_{oc}/E_g)*FF$, where QE is the quantum efficiency, F_0 is the overexcitation factor, or usable fraction of thermal radiation with energy greater than the diode bandgap, q is electron charge, V_{oc}/E_g is the open-circuit voltage V_{oc} factor based on the bandgap E_g of the diode material, and FF is the fill factor. Considering parameters that pertain specifically to diode performance, it was reported that theoretical limit values for QE, qV_{oc}/E_g, and FF are 1, 0.7, and 0.7, respectively[2].

Figure 1 schematically shows the p-on-n structure that has yielded high-performance TPV cells grown by OMVPE[6-9]. It consists of a thicker p-type emitter layer compared to the n-type base layer and an AlGaAsSb or GaSb window layer, and GaSb contact layer. This structure is used because shallow n-type contacts are difficult to prepare on GaSb-based materials and because of the larger minority carrier diffusion length in the p-type alloy compared to that in the n-type alloy. Surface recombination is detrimental to device performance[6], and both AlGaAsSb and GaSb window layers have been shown to be effective in reducing interfacial recombination velocity[9]. Figure 2 shows the spectral response for an uncoated GaInAsSb/AlGaAsSb/GaSb TPV cell[7]. The external QE (EQE) is approaching the theoretical limit and has response out to 2.5 μm. A summary of the peak value of EQE, V_{oc}, and FF for uncoated TPV cells fabricated from TPV cells grown over a period of several years is shown in Figures 3a, 3b, and 3c. It should be noted that the data presented in Figure 3 are taken from cells in which the alloy composition, emitter layer thickness, emitter and base layer doping levels, window layers, and device fabrication techniques had been intentionally varied in an effort to study parameters influencing diode performance. In general, the performance is relatively constant. The EQE and FF approach the theoretical limits, while the voltage factor is a maximum of 0.6. These results indicate that diode efficiency could be improved with increases in V_{oc}.

Enhancements in V_{oc} above existing values will require longer recombination lifetimes, a materials parameter that is sensitive to material defects, impurities, and surface properties[10]. Consequently, it is important to optimize the bulk material quality and epitaxial interfaces. Further improvements may be achieved by utilizing a reflector to enhance photon recycling effects in GaInAsSb[11]. This paper reports ongoing efforts to identify factors that can impact minority-carrier lifetime. Extensive materials studies were performed to optimize the quality of bulk GaInAsSb epitaxial layers and heterointerfaces grown by OMVPE. In addition, potential improvements in performance through the use of distributed Bragg reflectors[12] (DBRs) and back-surface reflectors[13] (BSRs) were studied.

MATERIALS STUDIES

Several factors that impact the bulk quality of epitaxial GaInAsSb alloys have been identified. These include properties of GaSb substrates and OMVPE growth parameters. Growth of high-quality epitaxial layers requires high-quality substrates, which serve as the template for subsequent crystal growth. Since GaSb-based materials are less developed compared to GaAs- and InP-based materials, the availability of high-

quality GaSb substrates has been more limited. GaSb is a softer material than either GaAs or InP, and as a result, substrates are more susceptible to damage during cutting, lapping, and polishing. As a result, the wafer bow in GaSb substrates is typically 10 µm, which is considerably larger compared to a only a few microns for GaAs. In addition, SiO_2 particles, which are used in substrate polishing, can become imbedded in the GaSb surface. Any surface contamination will result in surface defects in the epitaxy.

All substrates have gallium and antimony native oxides that must be removed before epitaxy. The oxides can be either thermally evaporated in the growth chamber or chemically etched before introduction into the chamber. Chemical etchants can be selected to remove only the oxides or both the oxides and GaSb. Atomic force microscopy images of the surface morphology of GaSb grown on an epi-ready substrate, where the oxide removal was performed by thermal evaporation, and on an etched substrate, where oxide and GaSb removal was by chemical etching are shown in Figures 4a and 4b, respectively. The morphology is rougher for the sample where the oxide was thermally evaporated, and is due to roughening of the surface during oxide desorption[14]. GaSb is consumed through a thermally activated chemical reaction between antimony oxide and GaSb. There is negligible oxide on an etched substrate and therefore, a smoother starting surface before epitaxy is achieved. Epitaxial growth of GaInAsSb was more sensitive to substrate preparation than growth of GaSb. The surface morphology of the GaInAsSb is smoother when only the oxides are chemically etched (Figure 4c) compared to that when the oxides and GaSb are etched (Figure 4d). Additional chemical etching of GaSb roughens the substrate surface. Surface roughness enhances adatom surface diffusion, which in turn can promote phase separation in GaInAsSb[15]. Phase separation in GaInAsSb results in localized microscopic regions that are GaAs- and InSb-rich, and this inhomogeneity can degrade structural and electro-optical quality, and thus reduce recombination lifetimes.

Phase separation can be effectively limited by growth kinetics such as growth temperature, growth rate, and substrate orientation. Excellent structural and optical properties were measured by x-ray diffraction and photoluminescence (PL), respectively[9,15]. Phase separation, however, cannot be completely eliminated because of thermodynamics, and an unusual manifestation of phase separation was observed in these materials. Figure 5 shows a cross-section transmission electron microscopy image of a natural superlattice (NSL) that spontaneously formed at the onset of GaInAsSb growth. The observed contrast arises from a very small degree of strain associated with a modulation in composition in the vertical direction. The contrast, and thus compositional differences between the layers, depended on the growth conditions and the alloy composition. It was found that the vertical composition modulation could be reduced or enhanced by varying the growth conditions.

PL measurements at 4 and 300 K are shown in Figures 6a and 6b for GaInAsSb that exhibited either a weak or strong NSL, respectively. Composition modulation is expected to increase the PL full width at half-maximum (FWHM) because local variations in alloy composition are associated with different bandgaps. However, the

results indicate that the broadening is minimal. The sample with a weak NSL has excellent PL properties with FWHM of 4.3 meV, and the dependence of the PL peak energy on temperature is typical of bulk materials and superlattices with a type-I band alignment. On the other hand, the sample with a strong NSL exhibits a slight broadening with FWHM of 9.5 meV. This increase could be due to either layer thickness variations in the NSL or spinodal decomposition. The dependence of the PL peak energy on temperature is similar to what is observed for type-II band alignment[16]. Type-II alignment can enhance minority carrier lifetime since electron and holes are spatially separated[17].

Previously, it was suggested that the dominant bulk recombination mechanism in GaInAsSb is not limited by Shockley-Read-Hall recombination, but likely by radiative and/or Auger recombination[18,19]. The electron lifetime of p-GaInAsSb doped at 2×10^{17} cm^{-3} was measured by time-resolved PL[20]. Double-heterostructures with different GaInAsSb thicknesses were grown in order to separate the contributions of bulk and interfacial recombination processes according to the equation $1/\tau_{PL} = 1/\tau_{BLK} + 2S/W$, where τ_{PL} is the PL decay, τ_{BLK} is a bulk lifetime, S is the surface recombination velocity which is assumed to be equal at the front and back heterointerfaces, and W is the active layer thickness. Three sets of samples were grown, each with different capping layers: nominally undoped p-GaSb (1×10^{16} cm^{-3}), p-GaSb (2×10^{18} cm^{-3}) and p-AlGaAsSb (2×10^{17} cm^{-3}). The results are shown in **Figure 7.** **All three plots demonstrate** a linear dependence consistent with the equation. The structures with undoped p-GaSb cap layers resulted in the highest S of 3100 cm/s. In structures with p-GaSb cap layers doped to 2×10^{18} cm^{-3}, S was substantially smaller at 1140 cm/s. Thus, the use of a heavily doped cap layer makes it possible to suppress interfacial recombination. S was further reduced to 720 cm/s for structures with AlGaAsSb cap layers. Higher S is due to accumulation of electrons at the GaInAsSb/GaSb type-II interface. Doping the cap layers reduces electron accumulation, while the AlGaAsSb cap layers results in no valence band offset[6]. Photon recycling can be significant and it can contribute to the slope and the offset. It was estimated that the contribution to the slope is about 200 cm/s to S for structures doped at 2×10^{17} cm^{-3}. The smallest S was 380 cm/s for undoped GaInAsSb with AlGaAsSb cap layers. In another set of samples, nominally undoped GaInAsSb ($p = 1 \times 10^{16}$ cm^{-3}) with undoped p-GaSb capping layers were evaluated. Here the contribution of the photon recycling is negligible, and a lower estimate of the bulk lifetime was determined to be 900 ns.

DEVICE STUDIES

Increases in minority-carrier lifetime are beneficial for TPV cell performance, and can be achieved through photon recycling. Two approaches are being studied: the use of either an integrated DBR or a BSR. Substrate absorption can reduce the effectiveness of a BSR[13], while increased series resistance can be problematic with DBR structures[19]. It is expected that either reflector can increase minority-carrier lifetime through photon recycling and provide double-pass absorption for photons that are not absorbed in the first pass. Enhanced QE especially near the bandedge of the

device is expected. The use of a reflector allows the emitter layer to be thinner, which should reduce the dark current.

For either approach, low series resistance contacts and high shunt resistance R_{SH} are critical for optimizing device performance. Ohmic contacts to n- and p-GaSb were formed by depositing Au/Sn/Ti/Pt/Au and Ti/Pt/Ag/PT/Au, respectively, and alloying the n-metal at 300°C. The p-type contacts were not alloyed. The specific contact resistivity ρ_c for n- and p-contacts on GaSb was measured by the Cox-Strack method. It was found that ρ_c for n- and p-contacts was 2.3×10^{-6} and 1.6×10^{-6} ohms-cm^2, respectively. It is slightly lower in the p-contacts than in the n-contacts because the Fermi level is pinned close to the valence band edge. Large-area (0.5 cm^2) TPV cells were fabricated using a conventional photolithographic process. A single 0.15-mm-wide central busbar connected to 10-μm-wide grid lines spaced 105 μm apart was used to make electrical contact to the front surface. TPV cells were defined by wafer sawing. The cutting introduces significant damage to the side walls and results in very low R_{SH} and degradation of FF. Saw-cut damage can be removed with chemical etching, and it was found that the R_{SH} could be increased from a few ohms to hundreds of ohms, while the values for FF increased from below 60% to 70%.

GaInAsSb/GaSb TPV structures were grown with and without a five-period AlGaAsSb/GaSb DBR tuned to have reflectivity centered at 2.4 μm. The 300 K PL spectra for the TPV control structure without a DBR and the DBR/TPV structure are shown in Figure 8a. The PL intensity is enhanced by about 40% due to photons reflecting from the DBR. The EQE of the uncoated TPV and DBR/TPV structures is shown in Figure 8b. No enhancement in EQE near the bandedge was observed, which may be due to the narrow bandwidth (~400 nm) of the DBR centered at 2.4 μm. It is expected that increased EQE may be possible for reflection centered at 2.2 μm. V_{oc} for the device with the DBR increased to 306 mV compared to 285 mV for the device without the DBR, or about 7%. Assuming a change only in recombination lifetime, a photon-recycling factor was estimated to be about 2.5. The series resistance for the TPV cell with the DBR is slightly higher at 1.2×10^{-2} Ω, compared to 0.8×10^{-2} Ω without the DBR. Grading and doping the interfaces in the DBR structure should reduce the series resistance[21].

GaInAsSb/GaSb TPV devices were also fabricated with a BSR. Free-carrier absorption in the n-GaSb substrate can be reduced by thinning the substrate[13], and a reflectivity of nearly 90% was measured for a substrate thinned to 100 μm thickness. A hybrid ohmic contact and BSR was constructed on the backside of a thinned and polished TPV cell. The EQE of an uncoated BSR-TPV device with substrate thickness of about 120 microns is in Figure 9. For comparison, the EQE of a conventionally processed TPV cell from the same wafer is also shown. The solid lines are guides for the eyes. The reflection limit of GaSb is also shown, in the dotted-dashed line. In the wavelength regime from about 1.1 to 1.7 μm, the BSR-TPV cell and the reference cell have approximately the same EQE since the GaSb substrate is absorbing below 1.7 mm. From about 1.7 to 2.5-μm, the EQE of the BSR-TPV cell exceeds that of the reference cell, and indicates the enhancement due to the double-pass absorption. The peak

difference in EQE is about 8% at a wavelength of 2.35 μm, which corresponds to a fractional increase in EQE of about 20% at this wavelength.

CONCLUSIONS

The optimization of GaInAsSb/(Al)Ga(As)Sb/GaSb TPV devices requires an extensive study of materials growth and characterization, device design, fabrication, and testing. High-performance TPV cells can routinely be fabricated, indicating good control and reproducibility of both epitaxial growth and device processing. Values of EQE and FF are approaching theoretical limits, while the voltage factor has remained fairly constant. Further improvements in the voltage factor should be forthcoming with increased understanding of recombination mechanisms in GaInAsSb. Preliminary device results on cells with an integral DBR structure indicate an increase in V_{oc}. Improvements in EQE was measured for TPV cells with a BSR.

ACKNOWLEDGMENTS

The authors gratefully acknowledge D.R. Calawa, J.W. Chludzinski, S. Hoyt, P.M. Nitishin, D.C. Oakley, and V.A. Todman of MIT Lincoln Laboratory for technical assistance. This work was sponsored by the Department of Energy under Air Force Contract No. F19628-00-C-0002. The opinions, interpretations, conclusions, and recommendations are those of the author and are not necessarily endorsed by the United States Air Force.

REFERENCES

1. P.F. Baldasaro, J.E. Raynolds, G.W. Charache, D.M. DePoy, C.T. Ballinger, T. Donovan, J.M. Borrego, 'Thermodynamic analysis of thermophotovoltaic efficiency and power density tradeoffs,' J. Appl. Phys. 89, 3319-3327 (2001).
2. G.W. Charache, J.L. Egley, D.M. DePoy, L.R. Danielson, M.J. Freeman, R.J. Dziendziel, J.F. Moynihan, P.F. Baldasaro, B.C. Campbell, C.A. Wang, H.K. Choi, G.W. Turner, S.J. Wojtczuk, P. Colter, P. Sharps, M. Timmons, R.E. Fahey, K. Zhang, 'Infrared Materials for Thermophotovoltaic Applications,' J. Electron. Mater. 27, 1038-1042 (1998).
3. Z.A. Shellenbarger, M.G. Mauk, J.A. Cox, M.I. Gottfried, P.E. Sims, J.D. Lesko, J.B. McNeely, L.C. DiNetta, R.L. Mueller, 'Improvements in GaSb-Based Thermophotovoltaic Cells,' AIP Conf. Proc. 401, 117-128 (1997).
4. O.V. Sulima, R. Beckert, A.W. Bett, J.A. Cox, M.G. Mauk, 'InGaAsSb photovoltaic cells with enhanced open-circuit voltage,' IEE Proc.-Optoelectron. 147, 199-204 (2000).
5. V.B. Khalfin, D.Z. Garbuzov, H. Lee, G.C. Taylor, N. Morris, R.U. Martinelli, J.C. Connolly, 'Interfacial Recombination in In(Al)GaAsSb/GaSb Thermophotovoltaic Cells,' AIP Conf. Proc. 460, 247-255 (1999).
6. H.K. Choi, C.A. Wang, G.W. Turner, M.J. Manfra, D.L. Spears, G.W. Charache, L.R. Danielson, D.M. DePoy, 'High-performance GaInAsSb thermophotovoltaic devices with an AlGaAsSb window,' Appl. Phys. Lett. 71, 3758-3760 (1997).

7. C.A. Wang, H.K. Choi, D.C. Oakley, G.W. Charache, 'Recent progress in GaInAsSb thermophotovoltaics grown by organometallic vapor phase epitaxy,' J. Cryst. Growth 195, 346-355 (1998).
8. C.A. Wang, H.K. Choi, S.L. Ransom, G.W. Charache, L.R. Danielson, D.M. DePoy, 'High-quantum-efficiency 0.5 eV GaInAsSb/GaSb thermophotovoltaic devices,' Appl. Phys. Lett. 75, 1305-1307 (1999).
9. C.A. Wang, H.K. Choi, G.W. Charache, 'Epitaxial growth of GaInAsSb for thermophotovoltaic devices,' IEE Proc.-Optoelectron. 147, 193-198 (2000).
10. S.M. Sze, *Physics of Semiconductors Devices* (John Wiley and Sons, New York), 1981.
11. J.M. Borrego, S. Saroop, R.J. Gutman, G.W. Charache, T. Donovan, P.F. Baldasaro, C.A. Wang, 'Photon recycling and recombination processes in 0.53 ev p-type InGaAsSb,' J. Appl. Phys. 89, 3753-3759 (2001).
12. S.P. Tobin, S.M. Vernon, M.M. Sanfacon, A. Mastrovito, 'Enhanced Light Absorption in GaAs Solar Cells with Internal Bragg Reflectors,' Proc. 22nd IEEE Photovoltaics Spec. Conf., 147-152 (1991).
13. G.W. Charache, D.M. DePoy, P.F. Baldasaro, B.C. Campbell, 'Thermophotovoltaic Devices Utilizing a Back Surface Reflector for Spectral Control,' AIP Conf. Proc. 321, 339-350 (1996).
14. C.J. Vineis, C.A. Wang, K.F. Jensen, 'In-situ reflectance monitoring of GaSb substrate oxide desorption,' J. Cryst. Growth 225, 420-425 (2001).
15. C.A. Wang, D.R. Calawa, C.J. Vineis, 'Evolution of surface structure and phase separation in GaInAsSb,' J. Cryst. Growth 225, 377-383 (2001).
16. N.N. Ledentsov, J. Bohrer, M. Beer, F. Heinrichsdorff, M. Grundmann, D. Bimberg, S.V. Ivanov, B.Ya. Meltser, S.V. Shaposhnikov, I.N. Yassievich, N.N. Faleev, P.S. Kop'ev, Zh.I. Alferov, 'Radiative states in type-II GaSb/GaAs quantum wells,' Phys. Rev. B 52, 14058-14066 (1995).
17. R.H. Ahrenkiel, S.P. Ahrenkiel, D.J. Arent, J.M. Olson, 'Carrier transport in ordered and disordered In0.53Ga0.47As,' Appl. Phys. Lett. 70, 756-758 (1997).
18. G.W. Charache, P.F. Baldasaro, L.R. Danielson, D.M. DePoy, M.J. Freeman, C.A. Wang, H.K. Choi, D.Z. Garbuzov, R.U. Martinelli, V. Khalfin, S. Saroop, J.M. Borrego, R.J. Gutman, 'InGaAsSb thermophotovoltaic diode: Physics evaluation,' J. Appl. Phys. 85, 2247-2252 (1999).
19. S. Saroop, J.M. Borrego, R.J. Gutman, G.W. Charache, C.A. Wang, 'Recombination processes in doubly capped antimonide-based quaternary thin films,' J. Appl. Phys. 86, 1527-1534 (1999).
20. D. Donetsky, C.A. Wang, S. Anikeev, G. Belenky, S. Luryi, G. Nichols, 'Reduction of the Interfacial Recombination Rate in GaInAsSb/GaSb Heterostructures,' 44th Electron. Mater. Conf., 26-28 June 2002, Santa Barbara, CA.
21. K.Tai, L. Yan, Y.H. Wang, J.D. Wynn, A.Y. Cho,'Drastic reduction of series resistance in doped semiconductor distributed Bragg reflectors for surface-emitting lasers,' Appl. Phys. Lett. 56, 2496-2498 (1990).

FIGURES

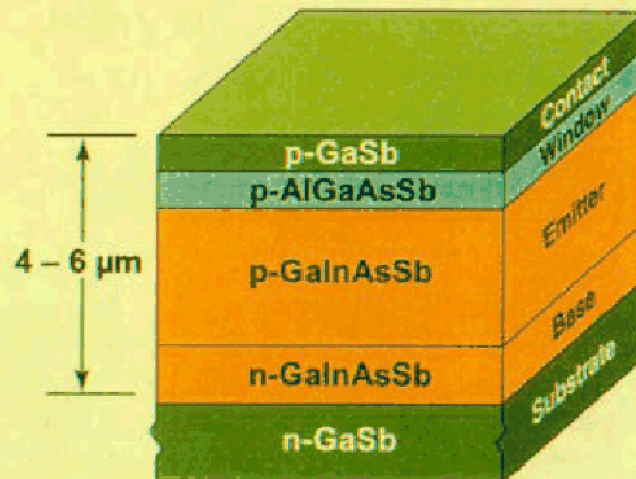

Figure 1. Schematic structure of GaInAsSb/AlGaAsSb/GaSb TPV device. The window layer can be either AlGaAsSb or GaSb.

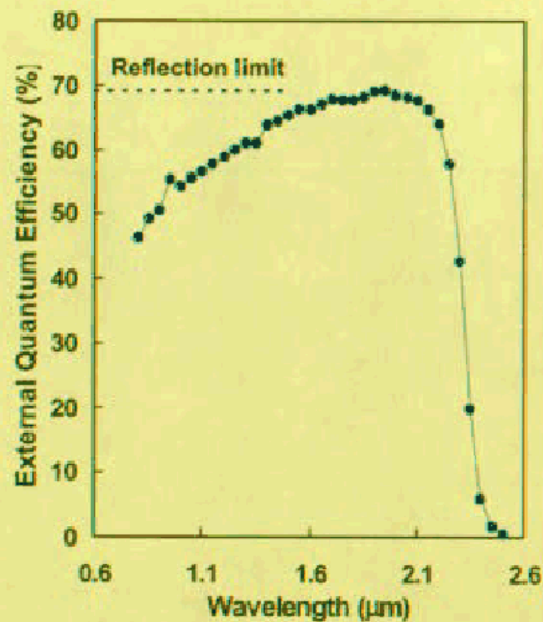

Figure 2. Spectral response of uncoated GaInAsSb/AlGaAsSb/GaSb TPV device.

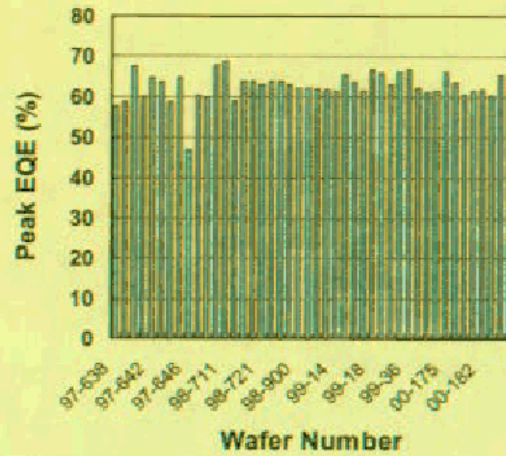

(a)

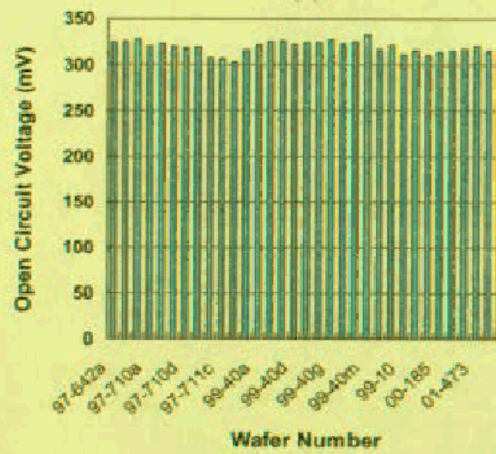

(b)

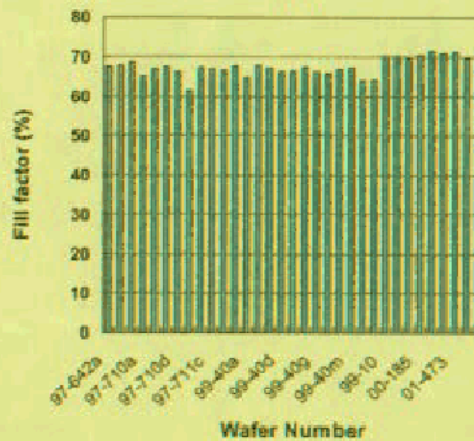

(c)

Figure 3. Device performance of GaInAsSb/(Al)Ga(As)Sb/GaSb TPV cells (0.5 or 1 cm^2) (a) peak external quantum efficiency; (b) open-circuit voltage; (c) fill factor.

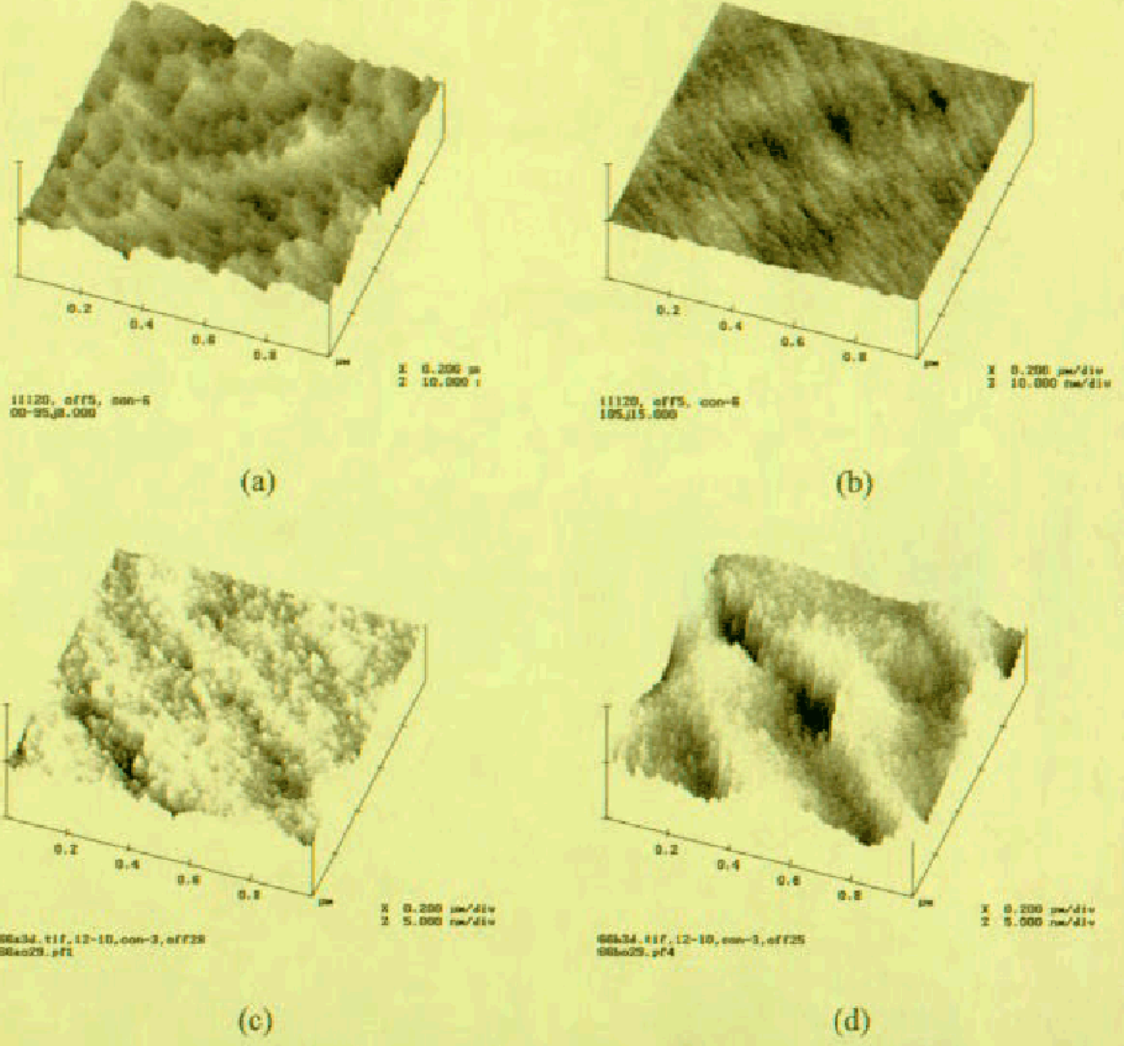

Figure 4. Atomic force microscopy images of (a) GaSb grown on epi-ready GaSb substrate; (b)GaSb grown on substrate etched to remove native oxides and GaSb; (c) GaInAsSb grown on substrate etched to remove native oxides and GaSb; (d) GaInAsSb grown on substrate etched to remove only native oxides.

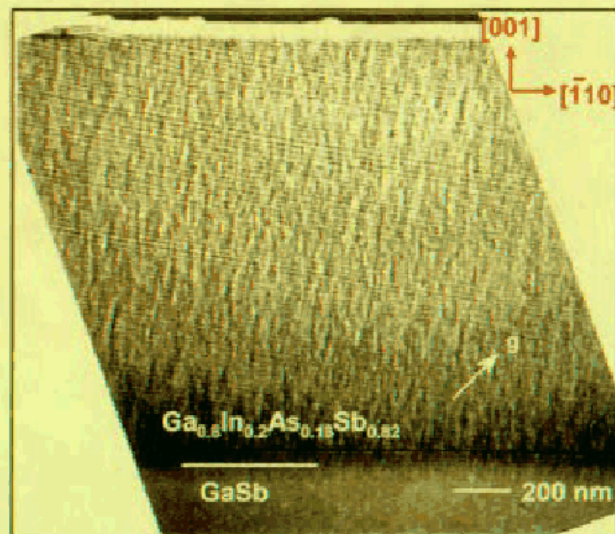

Figure 5. Cross-section transmission electron micrograph of natural superlattice formation in GaInAsSb.

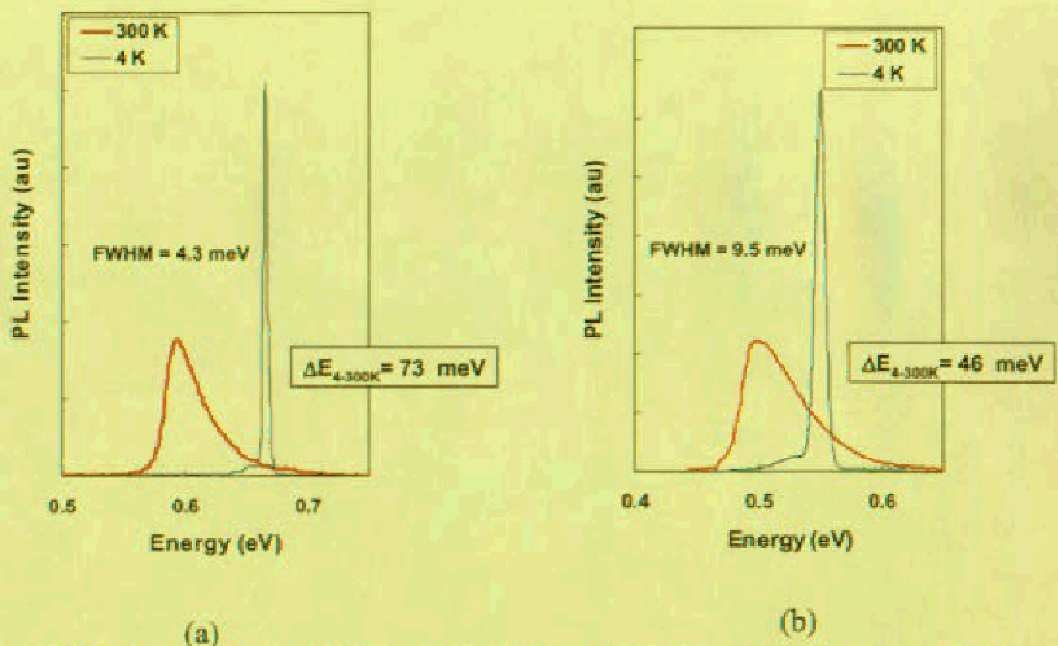

Figure 6. Photoluminescence of GaInAsSb: (a) sample with weak natural superlattice; (b) sample with strong superlattice.

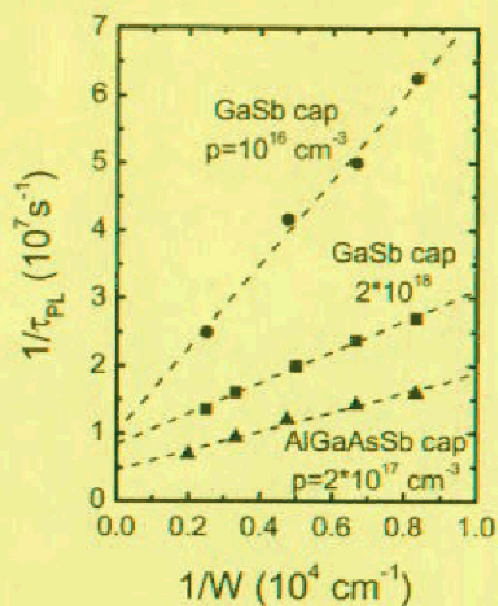

Figure 7. Inverse PL decay as a function of inverse thickness for three sets of GaInAsSb structures with different cap layers.

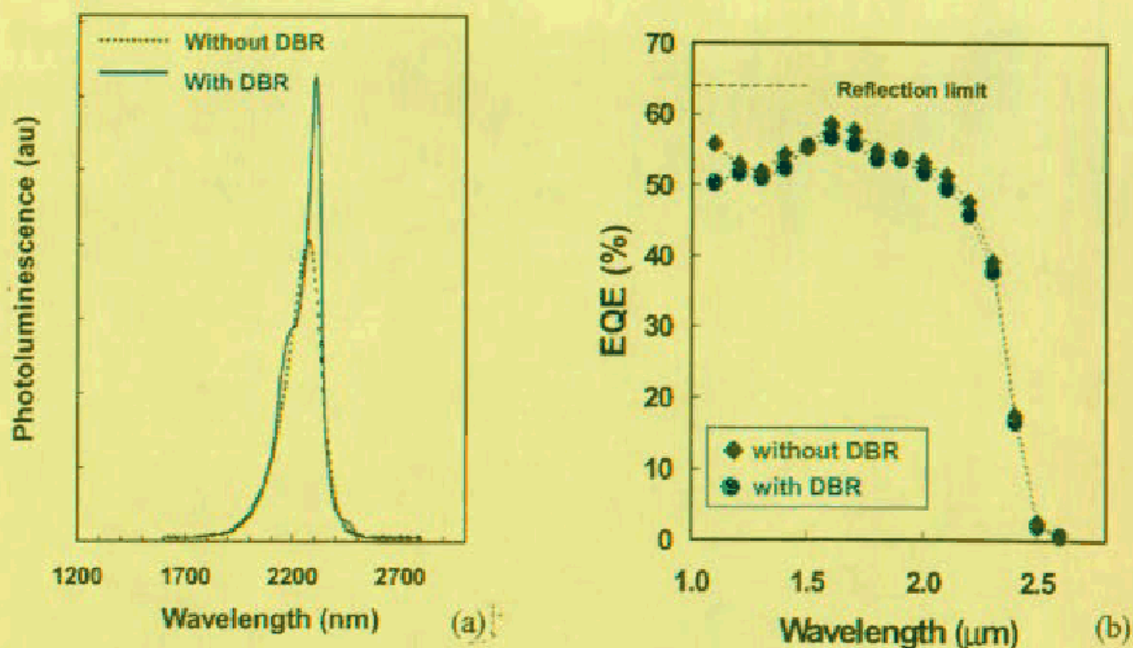

Figure 8. Comparisons of GaInAsSb/GaSb TPV devices with and without distributed Bragg reflector: (a) 300 K PL spectra; (b) external quantum efficiency.

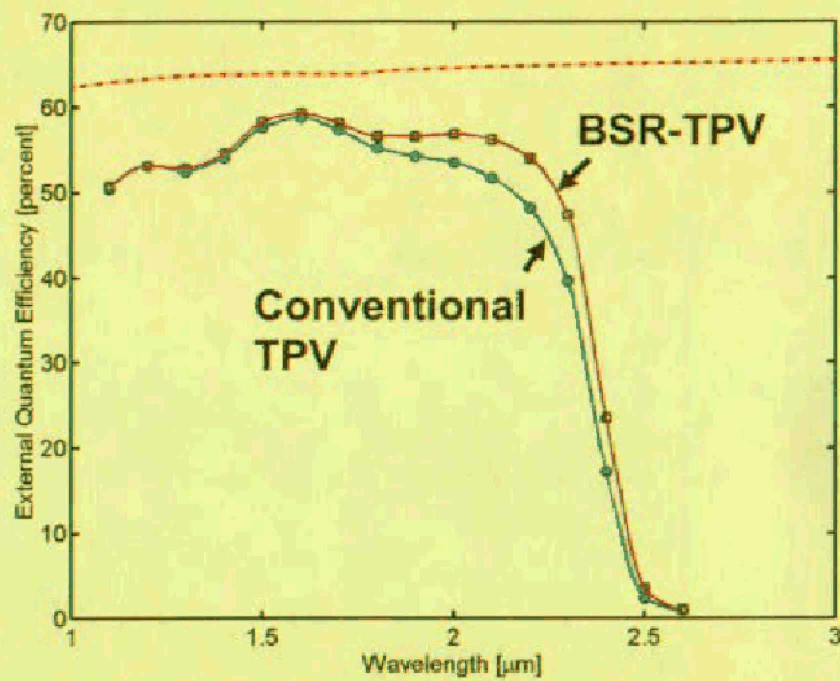

Figure 9. External quantum efficiency of GaInAsSb/GaSb TPV cells with and without back-surface reflector.